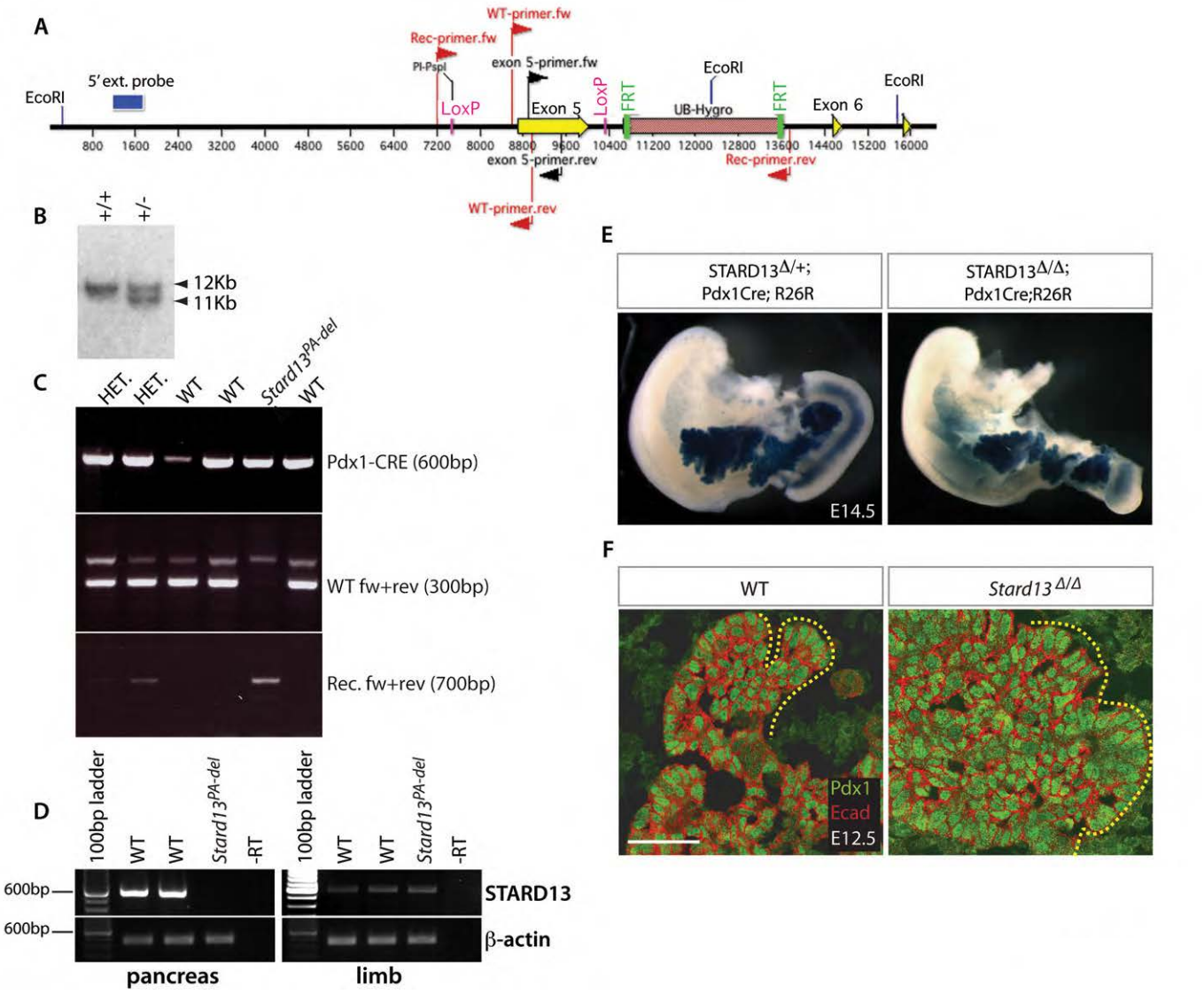

Fig. S1. Generation of pancreas-specific *Stard13*$^{PA\text{-}deleted}$ mice. (**A**) Schematic representation of the targeted *Stard13*^{flox} allele, indicating the loxP sites (in pink) flanking exon 5 of the gene, FRT-flanked-Hygromicin, *Eco*RI restriction sites, 5′ external probe (blue) and primers used for genotyping. Upon Cre-mediated recombination, excision of exon 5, which codes for amino acid residues 12-453, would fully inactivate the gene, introducing a frameshift mutation and premature stop codon, which results in a null *Stard13* allele. (**B**) Targeted ES cells and founder mice tails were identified by Southern blot analysis with restriction enzyme *Eco*RI and 5′ external probe. Upon digestion of genomic DNA with *Eco*RI, expected shift in size between WT (12.3 kb) and targeted (11.7 kb) allele was detected. (**C**) Deletion *in vivo* of the conditional allele in *Stard13*$^{flox/flox}$; *Pdx1-Cre* pancreatic cells. PCR on genomic DNA of E18.5 pancreatic rudiments for *Pdx1-Cre* transgene, wild-type (WT fw+rev primers) and recombined allele (Rec. fw+rev primers). In *Stard13*$^{PA\text{-}deleted}$ that carries the *Pdx1-Cre* transgene the recombined allele, but not the wild-type allele, was amplified, whereas the wild-type allele was detected in controls (HET or WT). (**D**) RT-PCR analysis of *Stard13* in pancreatic and forelimb tissue from WT and *Stard13*$^{PA\text{-}deleted}$ E14.5 embryos detected the transcript in both WT tissues, in the forelimb of *Stard13*$^{PA\text{-}deleted}$ embryos, but not in *Stard13*$^{PA\text{-}deleted}$ pancreas, indicating tissue-specific gene ablation. β-actin was used as control. (**E**) X-Gal staining in both *Stard13*$^{\Delta/+}$; *Pdx1-Cre*; ROSA26R$^{+/-}$ and *Stard13*$^{\Delta/\Delta}$; *Pdx1-Cre*; ROSA26R$^{+/-}$ indicated efficient Cre recombination, showing almost uniform blue staining in the pancreas at E14.5. R26R indicator mice were obtained from the Jackson Laboratory [Gt(ROSA)26Sortm1Sor] (Soriano, 1999). Pancreatic size difference was evident between HET and mutant. (**F**) Immunofluorescence analysis of E12.5 WT and *Stard13*$^{\Delta/\Delta}$ pancreases using antibodies against Pdx1 and E-cadherin (Ecad). Deletion of *Stard13* in all tissues (*Stard13*$^{\Delta}$) using the CMV-Cre transgenic strain (Schwenk et al., 1995) led to a pancreatic-specific phenotype as observed in *Stard13*$^{PA\text{-}deleted}$ embryos, suggesting a tissue-specific activity of the RhoGAP Stard13. Scale bar: 50 μm.

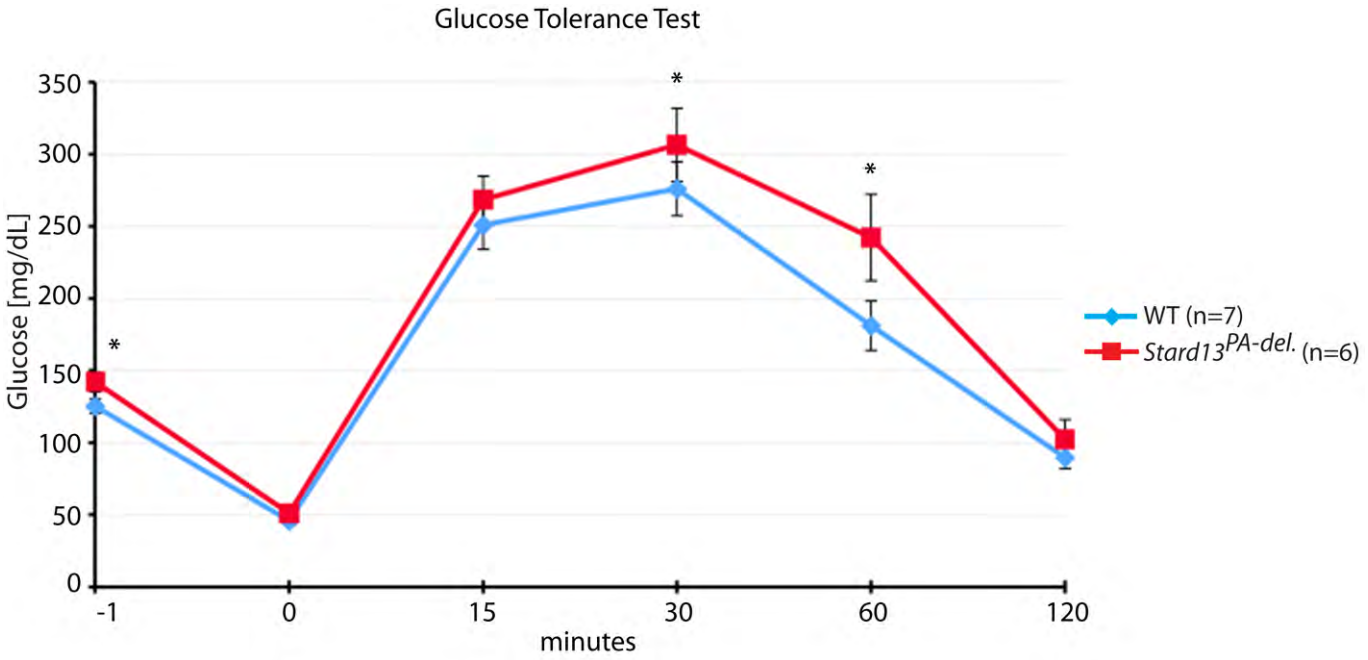

Fig. S2. Loss of *Stard13* leads to a mild glucose intolerance adult phenotype. Glucose levels were measured from blood collected from the tail immediately before the glucose challenge (time point 0) and 15, 30, 60 and 120 minutes after the glucose injection using a blood glucose meter (Contour, Bayer). Data are expressed as means ± s.e.m. The level of statistical significance was determined using Student's two-tailed *t*-test when the difference between the means of two populations was considered. $P<0.05$ was considered statistically significant. These results are in line with previous observations (Hammar et al., 2009). Finally, defects in glucose metabolism might explain the postnatal growth retardation that we observed in *Stard13*$^{PA\text{-}deleted}$ animals.

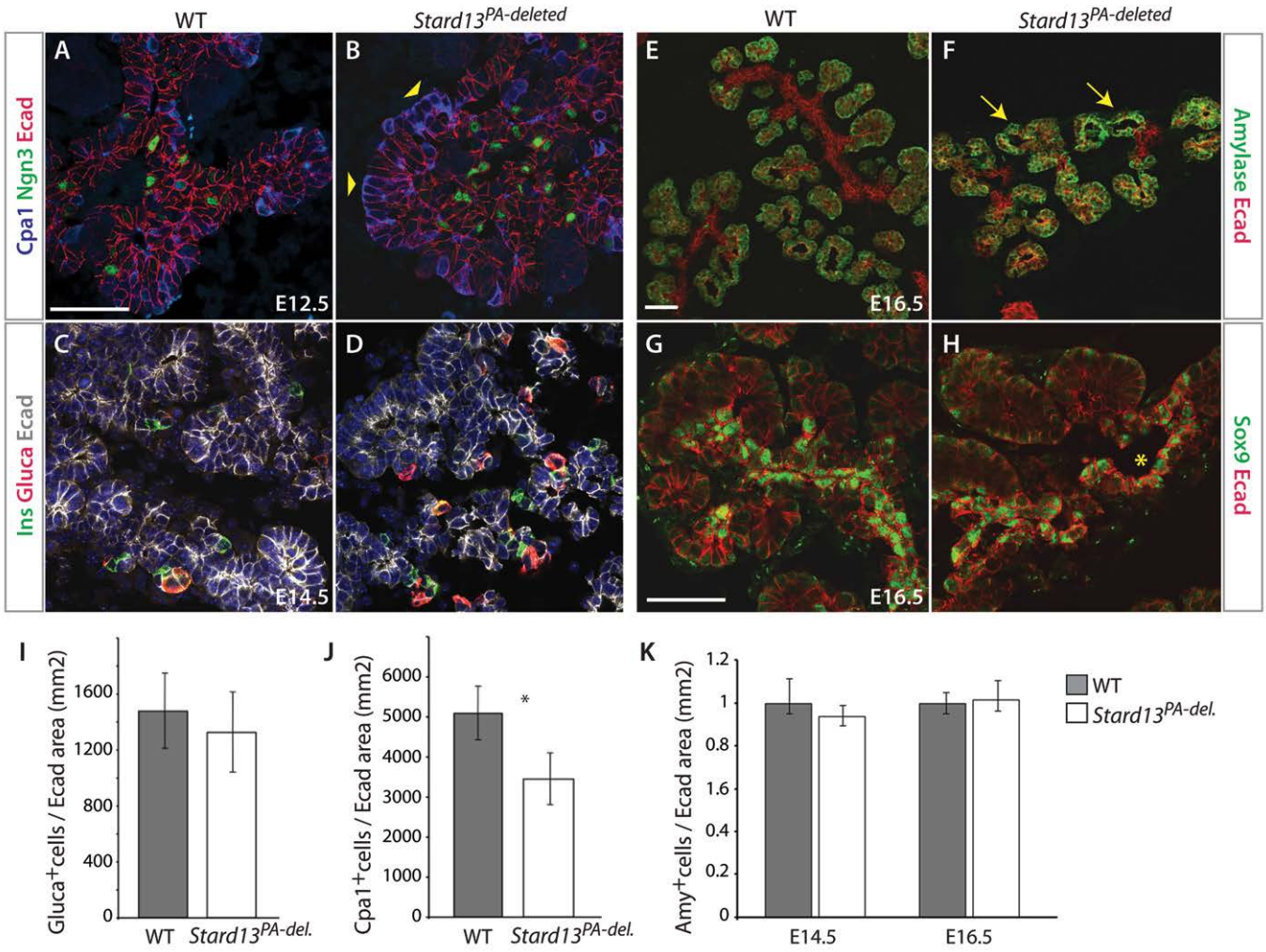

Fig. S3. *Stard13* ablation does not influence pancreatic lineage allocation. WT and *Stard13*$^{PA\text{-}deleted}$ pancreas sections were stained with antibodies against the three main pancreatic cell lineages. (**A**) The transcription factor *Ngn3* (*Neurog3*) is the earliest recognisable marker of endocrine progenitors, which subsequently give rise to mature endocrine cells. In the E12.5 WT, Ngn3+ (green) and Cpa1+ cells (blue) displayed typical distribution in the trunk and at the tips of the branching epithelium, respectively. (**B**) In the *Stard13*$^{PA\text{-}deleted}$ Ngn3+ cells trunk location was maintained, whereas Cpa1+ cells distribution was disorganised (arrowheads). (**C**,**D**) Endocrine cells expressing insulin (Ins) or glucagon (Gluca) cells were detected in both WT (C) and *Stard13*$^{PA\text{-}deleted}$ (D) E14.5 pancreases. Blue, Hoechst nuclear counterstain. (**E-H**) At E16.5, exocrine cells (amylase+) and duct cells (Sox9+) were found in both WT (E,G) and *Stard13*$^{PA\text{-}deleted}$ pancreases (F,H). Arrows indicate malformed acini (F) in the *Stard13*$^{PA\text{-}deleted}$ pancreas. The ductal network architecture was severely perturbed, showing discontinuous ducts (asterisk) and absence of typical branching tree-pattern in the mutant (H). (**I**) Quantification of differentiated endocrine cells (Gluca+) versus total Ecad+ area showed no change. *n*=3. (**J**) Quantification of progenitor Cpa1+ cells versus total Ecad+ area showed reduction in *Stard13*$^{PA\text{-}deleted}$ at E14.5, which is consistent with their decreased proliferative activity at E12.5 (Fig. 1F). Similarly, 30% reduction of Cpa1+ cells versus Pdx1+ cells was measured in the mutant pancreas (Cpa1+/Pdx1+cells in E14.5 *Stard13*$^{PA\text{-}deleted}$ pancreas=20±3.2 %; Cpa1+/Pdx1+cells in E14.5 WT pancreas=30±4 %). n=3. (**K**) No difference was observed in the relative number of exocrine cells (Amy+/Ecad+) between WT and *Stard13*$^{PA\text{-}deleted}$ pancreas at E14.5 and E16.5. *n*=3. Error bars represent ± s.e.m. **P*<0.05. Scale bars: 50 μm.

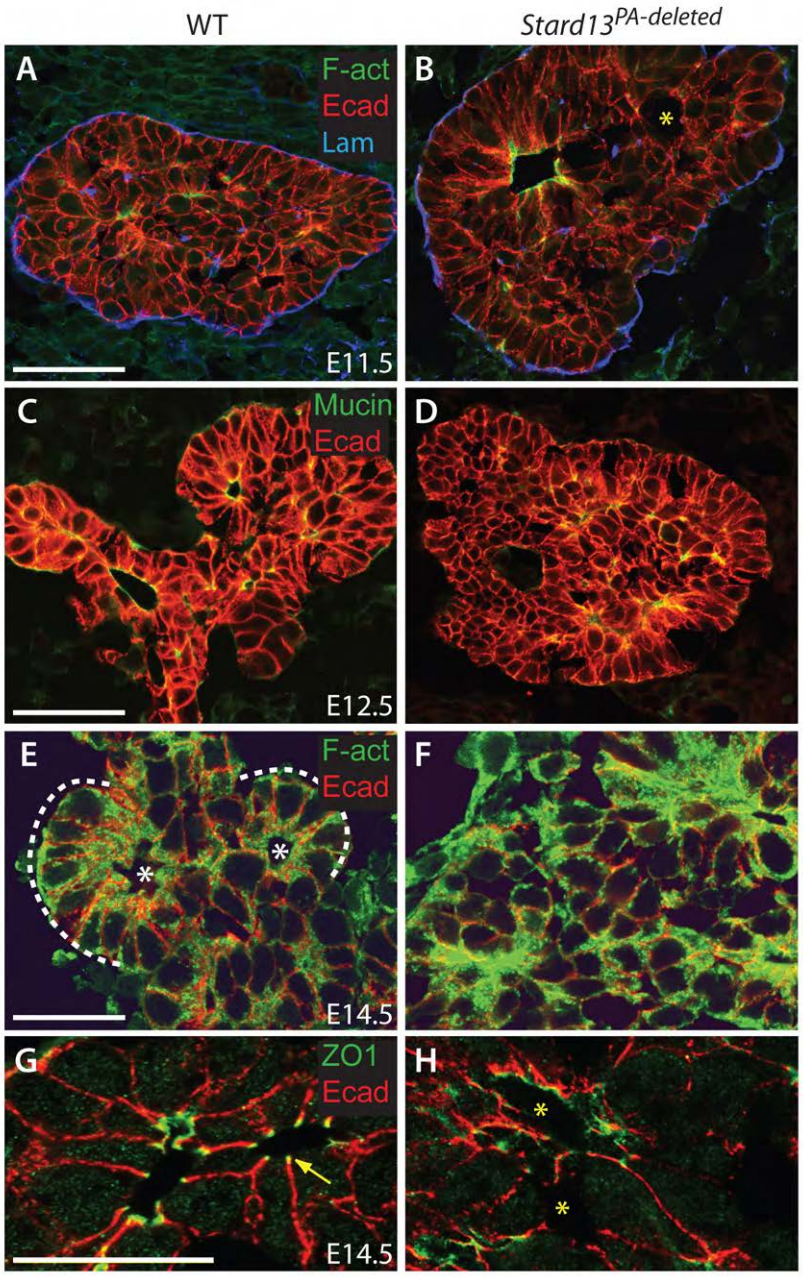

Fig. S4. Distribution of epithelial polarity markers in the developing pancreas. (**A**,**B**) WT and *Stard13*$^{PA\text{-}deleted}$ pancreatic sections were analysed for epithelial cell organisation with immunostaining for laminin (Lam), F-actin (F-act) and Ecad at E11.5. Microlumens were detected within the WT pancreatic epithelium and F-actin staining was properly distributed at the apical surface of the cells lining the lumens (A). In E11.5 *Stard13*$^{PA\text{-}deleted}$ pancreas, microlumens were not detected. By contrast, larger inner cavities surrounded by non-polarised cells with continuous E-cadherin membrane staining were found (B; asterisk). (**C**,**D**) Immunostaining for Mucin and Ecad at E12.5. *Stard13*$^{PA\text{-}deleted}$ cells display stratified and compact epithelial organisation with rare microlumens (D). (**E**,**F**) Immunostaining for F-act and Ecad at E14.5. *Stard13*$^{PA\text{-}deleted}$ cells display abnormal accumulation of F-actin (F). White outlines and asterisks indicate branches and lumens at E14.5, respectively (E). In the WT pancreas, F-actin filament meshwork normally underlay the apical pole, displaying a ratio of apical to basal mean fluorescence intensity between 1.5-1.6 A.U. on average, as measured by Image J. By contrast, in the absence of *Stard13* the measurable accumulation of F-actin at the basal pole is higher than in the control, resulting into a lower ratio of apical to basal mean fluorescence intensity (1.3-1.4 AU). This result suggests not only accumulation but also mislocalisation of the F-actin filaments in the absence of *Stard13*. (**G**,**H**) In E14.5 WT pancreatic epithelium, ZO-1 expression was detected at the apical edge of the junctional complex (arrow). In *Stard13*$^{PA\text{-}deleted}$ pancreas, newly forming lumens surrounded by either polarised or non-polarised cells were present (H). Asterisks indicate cavity surrounded by non-polarised cells. Scale bars: 50 μm (A-F); 20 μm (G,H).

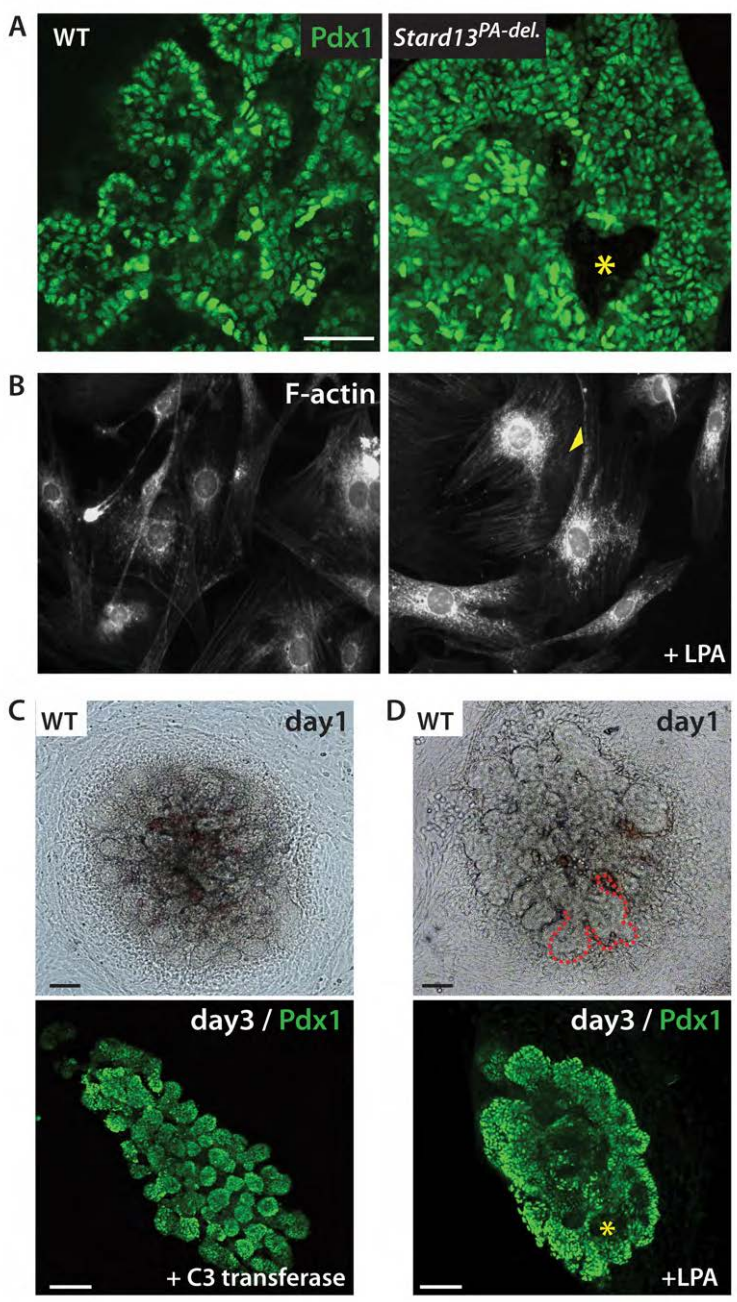

Fig. S5. Pharmacological activation or inhibition of the Rho signaling. (**A**) Whole-mount immunostaining for Pdx1 on WT explants showed tubules of Pdx1+ cells undergoing extensive branching by 48 hours of cultures. In *Stard13*$^{PA\text{-}deleted}$, pancreatic cells expressed Pdx1, but lacked tubules and typical branching organisation, as *in vivo*. Asterisk indicates internal cavity. (**B**) Activity of the LPA bioactive phospholipid was tested in embryonic fibroblast cultures using standard assays, such as staining of F-actin cytoskeleton with Alexa 488-phalloidin. Quiescent serum-starved mouse embryonic fibroblasts showed F-actin+ stress fibres. LPA treatment promoted flattening and increase in stress-fibre density (see yellow arrowhead), as result of RhoA activation. (**C**) Rho GTPase activity was selectively blocked through the use of a membrane-permeable version of the enzyme C3 transferase. E11.5 WT dorsal pancreases were cultured alone for 24 hours (day 1) and, subsequently, exposed to the C3 transferase during 48 hours. After 4 days, explants were fixed and immunostained with anti-Pdx1. C3 treatment did not perturb normal tubules formation and branching in WT developing pancreas. (**D**) In Rho activation assay, LPA was added at the final concentration of 10 μg/ml to the culture medium on day 1 and replaced every 24 hours. LPA-mediated activation of Rho reduced cell growth and antagonised tubulogenesis and branching in WT pancreatic epithelium, without affecting Pdx1 expression. Red outline indicates initiation of branching in WT pancreas organ culture after 24 hours in culture. Asterisk indicates internal cavities in LPA-treated explants. Scale bars: 50 μm (A); 100 μm (C,D).

Table S1. Primer sequences

Genotyping primers

Gene	Primer	Sequence	Size (bp)
WT Stard13	WT-fw	CAG TTC CAT GTT GGG TCT TCG T	259
	WT-rev.	CCT TCC AGC TGG GGG GTA GG	
Floxed Stard13 allele	Lox-fw	CAG TTC CAT GTT GGG TCT TCG T	330
	Lox-rev.	CCA GCT GGC TAG CTG GCA AAC	
Post-recombination product	Rec-fw.	CAG TTC CAT GTT GGG TCT TCG T	700
	Rec-rev.	AAC ATA CCT TAG ATC TAT TG	
Pdx1 Cre	Pdx1Cre-fw	tGC CAC GAC CAA GTG ACA GC	600
	Pdx1Cre-rev.	CCA GGT TAC GGA TAT AGT TCA TG	

RT-qPCR primers

Gene	Accession number	Primer	Sequence	Size (bp)
36B4	NM_007475.5	F	GGCCCTGCACTCTCGCTTTC	124
		R	TGCCAGGACGCGCTTGT	
SDHA	NM_023281.1	F	TGT TCA GTT CCA CCC CAC A	100
		R	TCT CCA CGA CAC CCT TCT GT	
Srf	NM_020493.2	F	GGCCGCGTGAAGATCAAGAT	159
		R	CACATGGCCTGTCTCACTGG	
Ctgf	NM_010217.2	F	CCCTAGCTGCCTACCGACT	113
		R	CATTCCACAGGTCTTAGAACAG G	
Vcl	NM_009502.4	F	GCAACCTCGTCCGGGTTGGAA	163
		R	TCCCGCGCAGGAACCGAGTA	
Mig6	NM_133753.1	F	TGGCCTACAATCTGAACTCCC	102
		R	GACCACACTCTGCAAAGAAGT	
β1-integrin	NM_010578.2	F	GGCGGACGCTGCGAAAAGATG A	160
		R	CCACCCACAATTTGGCCCTGCT	
α6-integrin	NM_008397.3	F	CGGTCTCCGGAGTCGCTAAGC	163
		R	TCAAGGTTGCTGTGCCGAGGTT	

Table S2. List of primary antibodies

Antibody	Raised in	Dilution	Source
Amylase	Rabbit	1:500	Sigma
Akt	Rabbit	1:1000	Cell Signaling
pAkt	Rabbit	1:1000	Cell Signaling
F-actin	FITC-conj.	1:500-1:750	Molecular Probes
Carboxypeptidase 1	Rabbit	1:500	AbD Serotec
E-cadherin	Rat	1:500-1:1000	Invitrogen
ERK1/2	Rabbit	1:1000	Cell Signaling
pERK1/2	Rabbit	1:1000	Cell Signaling
GAPDH	Rabbit	1:1000	Cell Signaling
Glucagon	Rabbit	1:500	Immunostar
GST	Rabbit	1:100	Santa Cruz
Phospho-Histone H3 (Er10)	Rabbit	1:200	Millipore
Insulin	Guinea pig	1:250	Millipore
Laminin	Rabbit	1:1000	Sigma
Mig6	Rabbit	1:100	Santa Cruz
Mucin	Armenian hamster	1:1000	Thermo Scientific
Phospho-MLC2	Rabbit	1:200	Cell Signaling
Neurogenin 3	Guinea pig	1:2000	Gift of M. Sander, UCSD, San Diego, CA, USA
Pdx1	Rabbit	1:2000	Abcam
Pdx1	Mouse	1:100	Hybridoma Bank
PKCζ	Rabbit	1:100	Santa Cruz
Ptf1a	Rabbit	1:2500	Gift of A. Sprinkler, BCBC Antibody Core, Novo Nordisk, Denmark
Sox-9	Rabbit	1:2000	Gift of M. Wegner, Erlangen University, Germany
YAP	Rabbit	1:100	Cell Signaling
p-YAP	Rabbit	1:100	Cell Signaling
ZO-1	Rabbit	1:100	Invitrogen